Synthesis and Reactivity of Mononuclear (Pentachlorophenyl)rhodium(II) Complexes. Structural Relevance of Rhodium−*o*-Chlorine Secondary Bonding

María P. García,* M. Victoria Jiménez, Angel Cuesta, Carmen Siurana, Luis A. Oro,* Fernando J. Lahoz, José A. López, and M. Pilar Catalán

Departamento de Química Inorgánica, Instituto de Ciencia de Materiales de Aragón, Universidad de Zaragoza-Consejo Superior de Investigaciones Científicas, 50009 Zaragoza, Spain

Antonio Tiripicchio and Maurizio Lanfranchi

Dipartimento di Chimica Generale ed Inorganica, Chimica Analitica, Chimica Fisica, Università di Parma, Centro di Studio per la Strutturistica Diffrattometrica del CNR, Viale delle Scienze 78, 43100 Parma, Italy

Received August 6, 1996[⊗]

Downloaded by CARLI CONSORTIUM on June 30, 2009
Published on March 4, 1997 on http://pubs.acs.org | doi: 10.1021/om960663i

The paramagnetic rhodium(II) complex $[PBzPh_3]_2[Rh(C_6Cl_5)_4]$ (**1a**) is obtained from the arylation of $[RhCl_3(tht)_3]$ with LiC_6Cl_5. Reaction of **1a** with CO affords the rhodium(I) complex $[PBzPh_3][Rh(C_6Cl_5)_2(CO)_2]$ (**2**). The oxidation of **1a** with chlorine or iodine gives the rhodium(III) compound $[PBzPh_3][Rh(C_6Cl_5)_4]$ (**3a**). The reaction of **3a** with methanolic solutions of HCl leads to the breaking of only one of the Rh−C bonds, producing the monomeric complex $[PBzPh_3][Rh(C_6Cl_5)_3Cl]$ (**4a**). Treatment of **3a** with potassium thiocyanate or thallium(I) acetylacetonate gives rise to the substitution of the chlorine ligand and to the formation of $[PBzPh_3][Rh(C_6Cl_5)_3X]$ (X = SCN, (**5**), acac (**6**)). With CO, **3a** yields the diacyl complex $[PBzPh_3][Rh\{C(O)C_6Cl_5\}_2(C_6Cl_5)Cl]$ (**7**). All the complexes are stable to the air and moisture in the solid state and moderately stable in deoxygenated solutions. The crystal structures of compounds **1a**, **3a**, **4a**, and **7** have been determined. Although these rhodium(II) or rhodium(III) complexes have four ligands, the coordination around the rhodium atoms is rather different, conforming in all cases to chiral molecular structures. Whereas complex **1a** shows an almost perfect square-planar geometry around the rhodium center, complexes **3a, 4a,** and **7** display distorted-octahedral environments. Two pentachlorophenyl groups in **3a** and one in **4a** behave as conventional σ-bonded ligands, while two additional C_6Cl_5 groups in **3a** and **4a** and one in **7** coordinate as chelating ligands, being bonded through the C_{ipso} atom and through *secondary bonding* interactions of the *o*-Cl atoms. Complex **7** additionally incorporates two (pentachlorophenyl)acyl groups linked as terminal or chelate ligands. The secondary-bonded *o*-chlorine atoms exhibit Rh−Cl distances in the range 2.5859−2.8863(9) Å.

Introduction

Although the most common oxidation states of rhodium are I and III, dimeric diamagnetic rhodium(II) compounds, metal−metal bonded, are numerous and are well-established.[1] However, relatively few monomeric species are known;[2] examples include coordination complexes of bulky phosphines[3] and sulfur[4] or nitrogen[5] donor ligands. The diverse reaction chemistry shown by rhodium(II) porphyrin complexes toward H_2, CO, and hydrocarbons[6] make this area of research particularly attractive.

As far as we are aware, there have been only three organometallic monomer rhodium(II) compounds structurally characterized; they are the neutral square-planar complexes $[Rh(2,4,6\text{-}^iPr_3C_6H_2)_2(tht)_2]$ (tht = tetrahydrothiophene),[7] $[Rh(C_6Cl_5)_2\{P(OPh)_3\}_2]$,[8] and the dication $[Rh(CN^tBu)_2(TMPP)_2]^{2+}$ (TMPP = tris(2,4,6-

[⊗] Abstract published in *Advance ACS Abstracts,* February 1, 1997.

(1) (a) Jardine, F. H.; Sheridan, P. S. In *Comprehensive Coordination Chemistry*; Wilkinson, G., Gillard, R. D., McCleverty, J. A., Eds.; Pergamon Press: Oxford, U.K., 1987; Vol. 4, p 930. (b) Livingstone, S. E. In *Comprehensive Inorganic Chemistry*; Bailar, J. C., Emeléus, H. J., Nyholm, R., Trotman-Dickenson, A. F., Eds.; Pergamon Press: Oxford, U.K., 1973; Vol. 3, Chapter 43. (c) Felthouse, T. M. *Prog. Inorg. Chem*. **1982**, *29*, 73. (d) Pruchnick, F. P. *Pure Appl. Chem*. **1989**, *61*, 795.

(2) For recent reviews see: (a) Bianchini, C.; Peruzzini, M.; Laschi, F.; Zanello, P. In *Topics in Physical Organometallic Chemistry*; Gielen, M. F., Ed.; Freund: London, 1991; Vol. 4, pp 139−220. (b) Pandey, K. K. *Coord. Chem. Rev*. **1992**, *121*, 1. (c) De Wit, D. G. *Coord. Chem. Rev*. **1996**, *147*, 209.

(3) (a) Haefner, S. C.; Dunbar, K. R.; Bender, C. *Organometallics* **1991**, *113*, 9540. (b) Dunbar, K. R.; Haefner, S. C.; Pence, L. E. *J. Am. Chem. Soc.* **1989**, *111*, 5504. (c) Harlow, R. L.; Thorn, D. L.; Barker, R. T.; Jones, N. L. *Inorg. Chem*. **1992**, *31*, 993.

(4) Cooper, S. R.; Rawle, S. C.; Yagbasan, R.; Watkin, J. *J. Am. Chem. Soc.* **1991**, *113*, 1600. Pandey, K. K.; Nehete, D. T.; Sharma, R. B. *Polyhedron* **1990**, *9*, 2013.

(5) Peng, S.; Peters, K.; Peters, E. M.; Simon, A. *Inorg. Chim. Acta* **1985**, *101*, L35.

(6) Wayland, B. B.; Ba, S.; Sherry, A. E. *J. Am. Chem. Soc.* **1991**, *113*, 5305. Wayland, B. B.; Ba, S.; Sherry, A. E. *Inorg. Chem*. **1992**, *31*, 148. Bunn, A. G.; Wei, M.; Wayland, B. B. *Organometallics* **1994**, *13*, 3390 and references therein.

(7) Hay-Motherwell, R. S.; Koschmieder, S. U.; Wilkinson, G.; Hussain-Bates, B.; Hursthouse, M. B. *J. Chem. Soc., Dalton Trans.* **1991**, 2821.

(8) García, M. P.; Jiménez, M. V.; Oro, L. A.; Lahoz, F. J.; Casas, J. M.; Alonso, P. J. *Organometallics* **1993**, *12*, 3257.

S0276-7333(96)00663-2 CCC: $14.00 © 1997 American Chemical Society

Downloaded by CARLI CONSORTIUM on June 30, 2009
Published on March 4, 1997 on http://pubs.acs.org | doi: 10.1021/om960663i

trimethoxyphenylphosphine).[9] In addition, the formally octahedral species $[Rh(np_3)(C{\equiv}CPh)]^+$ (np_3 = $N(CH_2CH_2PPh_2)_3$),[10] $[Rh(\eta^6\text{-}C_6Me_6)_2]^{2+}$,[11] and the square-planar $[Rh(C_6Cl_5)_2L_2]$ (L_2= cod, $\{P(OMe)_3\}_2$, $(PPh_3)_2$, $(py)_2$ (py = pyridine), dppe (dppe = 1,2-bis(diphenylphosphino)ethane), dppm (dppm = 1,2-bis(diphenylphosphino)methane)),[8] have been characterized by analytical and spectroscopical means and the short-lived rhodocene[12] and some cationic species electrochemically generated in solution[13] have been described.

During our work exploring the chemistry of perhalophenyl derivatives of rhodium[8,14] and iridium,[15] we have been able to prepare the first homoleptic mononuclear iridium(II) dianion $[Ir(C_6Cl_5)_4]^{2-}$, which has been fully characterized.[16] This type of binary complex has no parallel in rhodium(II) chemistry. Even with the binary halides, there is only some evidence for the existence of the dichloride $RhCl_2$, and although both the dibromide and diiodide have been reported, their existence is doubtful.[1b] Related compounds such as $[RhX_6]^{4-}$ (X = H, Cl, Br) and $[RhO_6]^{10-}$ are very unstable, and they have been studied by trapping them within a crystal lattice to extend their short lifetime.[2b]

On the other hand, it is known that the C_6Cl_5 anion stabilizes Rh and Ir complexes in the unusual oxidation state II, in the same way that it does with the oxidation state III of platinum[17] in the complex $(NBu_4)[Pt(C_6Cl_5)_4]$. Therefore, we sought the experimental conditions which allow the synthesis of homoleptic rhodium(II) compounds, isoelectronic with the aforementioned $[Ir^{II}(C_6Cl_5)_4]^{2-}$ and $[Pt^{III}(C_6Cl_5)_4]^-$.

In this paper we report the synthesis and full characterization of the homoleptic rhodium(II) aryl complex $[Rh(C_6Cl_5)_4]^{2-}$ and its two one-electron-oxidation products, the monoanions $[Rh(C_6Cl_5)_4]^-$ and $[Rh(C_6Cl_5)_3Cl]^-$, whose molecular structures are remarkably different from that of the parent dianion. Some guidelines of the reactivity of $[Rh(C_6Cl_5)_4]^{2-}$—leading to the preparation of different rhodium(III) oxidation products—are also presented together with an structural investigation of the molecular structure of the anions $[Rh(C_6Cl_5)_4]^-$, $[Rh(C_6Cl_5)_3Cl]^-$, and $[Rh\{C(O)C_6Cl_5\}_2(C_6Cl_5)Cl]^-$. The analysis of the metal coordination spheres reveals the existence of secondary-bonded chlorine atoms. A discussion of the nature and characteristics of this type of interaction is also presented on the basis of structural and theoretical data.

Results and Discussion

Synthesis and Reactivity of the Dianion $[Rh(C_6Cl_5)_4]^{2-}$ (1). The reactions of $[RhCl_3(tht)_3]$ with an excess of LiC_6Cl_5 (1:10 molar ratio), in diethyl ether at −50 °C, lead to solutions containing the arylated anion $[Rh(C_6Cl_5)_4]^{2-}$ (**1**), from which, by addition of the $[PBzPh_3]^+$ or $[NBu_4]^+$ cations and workup, the yellow microcrystalline solids $[PBzPh_3]_2[Rh(C_6Cl_5)_4]$ (**1a**) and $[NBu_4]_2[Rh(C_6Cl_5)_4]$ (**1b**) can be isolated.[18] During the arylating reaction, a one-electron-reduction process has taken place; a similar process has been described when the starting product $[RhCl_3(tht)_3]$ reacts with Li(2,4,6-^{i}Pr$_3$C$_6$H$_2$), yielding[7] the complex $[Rh(2,4,6\text{-}^iPr_3C_6H_2)_2(tht)_2]$. In fact, in the reactions of $[RhCl_3(tht)_3]$ with lithium derivatives, the nature and yield of the products depend on the experimental conditions and on the steric properties of the aryl or alkyl group used. Thus, with LiC_6F_5 it gives[14a] the square-pyramidal rhodium(III) dianion $[Rh(C_6F_5)_5]^{2-}$, with LiMe it affords[19] the octahedral $[RhMe_6]^{3-}$, and with Li(2,4,6-^{i}Pr$_3$C$_6$H$_2$) it provides[7] the neutral square-planar complex $[Rh(2,4,6\text{-}^iPr_3C_6H_2)_2(tht)_2]$. Radical reactions are probably involved in these transformations.

Compounds **1a** and **1b** are stable to the air in the solid state. In deoxygenated acetone solutions (approximately 5×10^{-4} M) they behave as 2:1 electrolytes.[20] Their stoichiometry was deduced from elemental analyses (C, H, and N), mass spectra and conductivity. The IR spectra (Experimental Section) exhibit absorptions due to the C_6Cl_5 groups[21] as well as to the cations. The monomeric nature of the anion, corresponding to a rhodium(II) center, as well as its square-planar geometry has been established by an X-ray structural determination of complex **1a**, which will be discussed later. The molecular geometry observed is in agreement with the EPR data; the compounds $[PBzPh_3]_2[Rh(C_6Cl_5)_4]$ (**1a**) and $[NBu_4]_2[Rh(C_6Cl_5)_4]$ (**1b**) are paramagnetic, and their X-band EPR spectra at room temperature are analogous to those found for the neutral Rh(II) complexes $[Rh(C_6Cl_5)_2L_2]$.[8] Figure 1 shows the EPR spectrum of complex **1b** in which the g values are $g_x = 2.74$, $g_y = 2.60$, and $g_z = 1.94$. These g values can be understood if the unpaired electron is mainly in a d_{z^2} orbital with the z axis perpendicular to the first coordination plane of the rhodium atom. No evidence of

(9) Dunbar, K. R.; Haefner, S. C. *Organometallics* **1992**, *11*, 1431.
(10) Bianchini, C.; Laschi, F.; Ottaviani, F.; Peruzzini, M.; Zanello, P. *Organometallics* **1988**, *7*, 1660.
(11) Fischer, E. O.; Lindner, H. H. *J. Organomet. Chem.* **1964**, *1*, 307.
(12) Fischer, E. O.; Wawersick, H. *J. Organomet. Chem.* **1966**, *5*, 559. Keller, H. J.; Wawersick, H. *J. Organomet. Chem.* **1967**, *8*, 185.
(13) Dessy, R. E.; King, R. B.; Waldrop. M. *J. Am. Chem. Soc.* **1966**, *88*, 5112. Pilloni, G.; Schiavon, G.; Zotti, G.; Zecchin, S. *J. Organomet. Chem.* **1977**, *134*, 305. Bianchini, C.; Laschi, F.; Meli, A.; Peruzzini, M.; Zanello, P.; Frediani, P. *Organometallics* **1988**, *7*, 2575. Bianchini, C.; Herrera, V.; Jiménez, M. V.; Laschi, F.; Meli, A.; Sanchez-Delgado, R.; Vizza, F.; Zanello, P. *Organometallics* **1995**, *14*, 4390.
(14) (a) García, M. P.; Oro, L. A.; Lahoz, F. J. *Angew. Chem.* **1988**, *100*, 1766; *Angew. Chem., Int. Ed. Engl.* **1988**, *27*, 1700. (b) García, M. P.; Jiménez, M. V.; Lahoz, F. J.; Oro, L. A.; Tiripicchio, A.; Lopez, J. A. *J. Chem. Soc., Dalton Trans.* **1990**, 1503. (c) García, M. P.; Jiménez, M. V.; Lahoz, F. J.; Oro, L. A. *J. Chem. Soc., Dalton Trans.* **1995**, 917. (d) García, M. P.; Jiménez, M. V.; Oro, L. A. *J. Organomet. Chem.* **1992**, *438*, 229.
(15) (a) García, M. P.; Jiménez, M. V.; Lahoz, F. J.; Oro, L. A. *Inorg. Chem.* **1995**, *34*, 2153. (b) García, M. P.; Jiménez, M. V.; Oro, L. A.; Lahoz, F. J.; Alonso, P. J. *Angew. Chem.* **1992**, *104*, 1512; *Angew. Chem., Int. Ed. Engl.* **1992**, *31*, 1527.
(16) García, M. P.; Jiménez, M. V.; Oro, L. A.; Lahoz, F. J.; Camellini Tiripicchio, M.; Tiripicchio, A. *Organometallics* **1993**, *12*, 4660.
(17) (a) Usón, R.; Forniés, J.; Tomás, M.; Menjón, B.; Sünkel, K.; Bau, R. *J. Chem. Soc., Chem. Commun.* **1984**, 751. (b) Usón, R.; Forniés, J.; Tomás, M.; Menjón, B.; Bau, R.; Sünkel, K.; Kuwabara, E. *Organometallics* **1986**, *5*, 1576.
(18) The anions described in this paper have been crystallized with $PBzPh_3^+$ cations; this cation has proved to be adequate to grow suitable crystals for the X-ray determinations. However, the IR spectra in the 600 and 800 cm^{-1} regions, as well as the ^{13}C NMR spectra, cannot be properly studied with this cation as the counterion, because the absorptions of the phenyl rings of the cation overlap with those of the C_6Cl_5 rings. For this reason, some NBu_4^+ salts have also been prepared and characterized. In the compounds prepared with both cations, the anions have been numbered as: $[Rh(C_6Cl_5)_4]^{2-}$ (**1**), $[Rh(C_6Cl_5)_4]^-$ (**3**), and $[Rh(C_6Cl_5)_3Cl]^-$ (**4**) and the suffixes **a** and **b** have been used for the complexes with the $PBzPh_3^+$ and NBu_4^+ cations, respectively.
(19) Hay-Motherwell, R. S.; Wilkinson, G.; Hussain-Bates, B.; Hursthouse, M. B. *J. Chem. Soc., Chem. Commun.* **1989**, 1436. Hay-Motherwell, R. S.; Wilkinson, G.; Hussain-Bates, B.; Hursthouse, M. B. *Polyhedron* **1990**, 2071.
(20) Geary, W. J. *Coord. Chem. Rev.* **1971**, *7*, 81.
(21) Maslowsky, E. *Vibrational Spectra of Organometallic Compounds;* Wiley: New York, 1977; p 437.

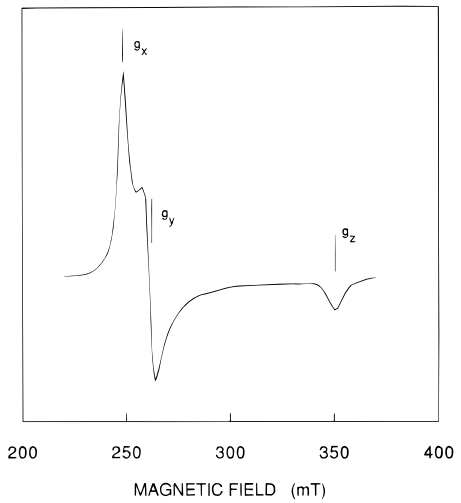

Figure 1. EPR spectrum of the rhodium(II) complex $[NBu_4]_2[Rh(C_6Cl_5)_4]$ (**1b**): powdered sample measured at room temperature.

hyperfine (HF) structure has been found in any of the spectra of these compounds.

Reduction of $[Rh(C_6Cl_5)_4]^{2-}$ with Carbon Monoxide. Bubbling CO through a CH_2Cl_2 suspension of $[PBzPh_3]_2[Rh(C_6Cl_5)_4]$ (**1a**) at 1 atm of pressure and room temperature gives a yellow solution from which, after workup, $[PBzPh_3][Rh(C_6Cl_5)_2(CO)_2]$ (**2**) is obtained (yield 43%). The IR spectra of **2** exhibit, in CH_2Cl_2 solution or in the solid state, two ν(CO) bands characteristic of *cis*-dicarbonylrhodium(I) complexes. The EPR spectrum of the complex shows no signals. The analytical data, mass spectrum (FAB), and conductivity (1:1 electrolyte) confirm that a one-electron-reduction process has taken place and that the *cis* rhodium(I) complex $[Rh(C_6Cl_5)_2(CO)_2]^-$ has been formed. This known complex[8] is also obtained by reaction of the rhodium(I) dimer $[\{Rh(\mu\text{-}Cl)(CO)_2\}_2]$ with $Li[C_6Cl_5]$.

Oxidation of $[Rh(C_6Cl_5)_4]^{2-}$ with Chlorine or Iodine. Synthesis of $[Rh(C_6Cl_5)_4]^-$ (3). Being a rhodium(II) compound, complex **1** reacts with chlorine or iodine, affording rhodium(III) derivatives. Treatment of acetone solutions of the remarkably stable rhodium(II) complexes **1a** and **1b** with carbon tetrachloride solutions of chlorine (1:1 molar ratio) leads to the isolation of $[PBzPh_3][Rh(C_6Cl_5)_4]$ (**3a**) and $[NBu_4][Rh(C_6Cl_5)_4]$ (**3b**) (eq 1). The C, H, and N analyses, the

$$[Rh(C_6Cl_5)_4]^{2-} + {}^1/_2Cl_2 \rightarrow [Rh(C_6Cl_5)_4]^- + Cl^- \quad (1)$$

conductivity measurements (1:1 electrolyte), and the mass spectra are in agreement with the proposed formulation. The EPR spectra of solid samples of **3a** or **3b** show no signals in accord with the d^6 configuration of the Rh^{III} metal center.

Complex **1** also reacts with iodine. In this case an excess of the oxidant is necessary to complete the reaction. Treatment of compound **1a** with iodine in CH_2Cl_2 (molar ratio 1:2.5), at room temperature, provides a brown solution from which a reddish solid is obtained. Crystallization of this solid by slow diffusion of hexane into a CH_2Cl_2 solution produces two different compounds: the orange crystalline complex **3a** and dark red crystals, identified by their spectra and elemental analysis as $[PBzPh_3][I_3]$ (eq 2).

Scheme 1

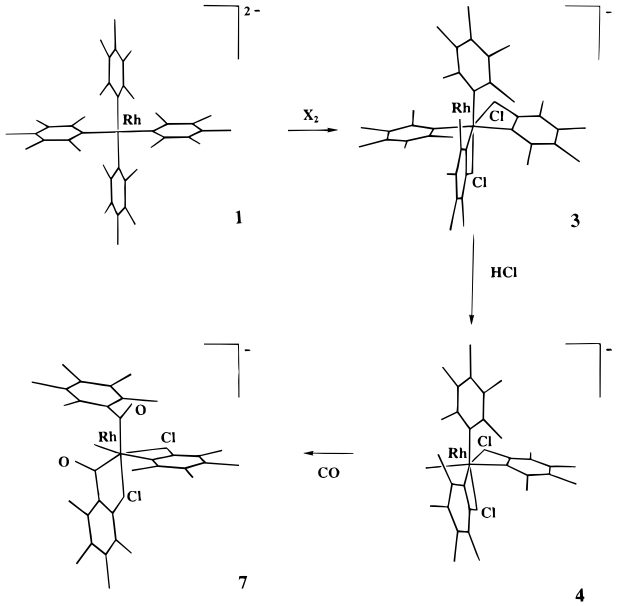

$$[PBzPh_3]_2[Rh(C_6Cl_5)_4] + {}^3/_2I_2 \rightarrow [PBzPh_3][Rh(C_6Cl_5)_4] + [PBzPh_3][I_3] \quad (2)$$

From the mixture of the crystals, both complexes can be separated due to their different solubilities in diethyl ether; thus, when this solvent is diffused into a CH_2Cl_2 solution of the mixture only crystals of $[PBzPh_3][I_3]$ are obtained, while complex **3a** remains in solution.

The structure of **3a**, studied by X-ray crystallography, shows that in the monoanion $[Rh(C_6Cl_5)_4]^-$ the rhodium atom is six-coordinated, in contrast to the four-coordinated rhodium(II) of the dianion $[Rh(C_6Cl_5)_4]^{2-}$. The rhodium atom, in **3a**, is located in a distorted-octahedral environment formed by four Rh−C σ-bonds and two Rh−Cl interactions, involving two *o*-chlorine atoms of two C_6Cl_5 groups. The structural change (Scheme 1) occurring from the dianion $[Rh(C_6Cl_5)_4]^{2-}$ to the monoanion $[Rh(C_6Cl_5)_4]^-$ can be observed, in the IR spectra, from the C_6Cl_5 absorptions in the 1300 cm^{-1} region; while the square-planar rhodium(II) complex **1** presents only two strong bands, the octahedral complex **3** shows four separated absorptions, indicating the differences in the coordination of the pentachlorophenyl groups. The absorptions at *ca.* 600 and *ca.* 800 cm^{-1}, which can be assigned to ν(M−C) and the X-sensitive vibration modes of the C_6Cl_5 ligands, respectively, are affected by the oxidation state of the metal center. Thus, the increase in the oxidation state from Rh(II) to Rh(III) is reflected in the higher values of the wavenumber observed for both ν(Rh−C) and the X-sensitive modes. The Experimental Section gives the absorption bands observed for the complexes in these regions, which mostly coincide with the expected ones.

Complex **3** presents, in the solid state, two Rh−Cl interactions; to check if these interactions are retained in solution, we have measured the ^{13}C NMR spectra of $[NBu_4][Rh(C_6Cl_5)_4]$ (**3b**) at different temperatures (Table 1). From +20 to −80 °C, only one set of signals for the different C atoms of the C_6Cl_5 rings is observed. This behavior suggests that, in solution, either the Rh−Cl

Downloaded by CARLI CONSORTIUM on June 30, 2009
Published on March 4, 1997 on http://pubs.acs.org | doi: 10.1021/om960663i

Table 1. ^{13}C NMR Data (δ, ppm) for Complexes 3−5

	$(NBu_4)[Rh^{III}(C_6Cl_5)_4]$ (**3b**)	$(NBu_4)[Rh^{III}(C_6Cl_5)_3Cl]$ (**4b**)	$(PBzPh_3)[Rh^{III}(C_6Cl_5)_3SCN]$ (**5**)
20 °C, $CDCl_3$			
ipso C	146.9 (d, $^1J_{Rh-C}$ = 43.7 Hz)	137.3 (d, $^1J_{Rh-C}$ = 49.6 Hz)	137.4 (d, $^1J_{Rh-C}$ = 48.2 Hz)
ortho C	140.7 (s)	139.5 (s)	139.6 (s)[a]
meta C	126.8 (s)	127.6 (fd, ^3J = 2.5 Hz)	*d*
para C	127.5 (s)	126.8 (s)	*d*
−55 °C, $CDCl_3$			
ipso C	not obsd	137.1 (m)[b]	
ortho C	140.8 (m)[a]		
meta C	127.1 (m)	127.3 (m)[c]	
para C	127.8 (m)		
−80 °C, CD_2Cl_2			
ipso C	not obsd	137.5 (d, $^1J_{Rh-C}$ = 48.2 Hz), 138 (m)[a]	138.7 (d, $^1J_{Rh-C}$ = 73.8 Hz), 136.3 (d, $^1J_{Rh-C}$ = 57.8 Hz)
ortho C	142 (m)[a]	144.4 (m), 139 (m)[a]	144.6 (s), 142.4 (s)
meta C	128 (m)[a]	128.1 (m), 128.8 (m)[a]	*d*
para C	126.2 (m)	126.3 (m), 127.3 (m)[a]	*d*

[a] Broad signals. [b] Broad signals including ipso C and ortho C. [c] Broad signals including meta C and para C. [d] Included in the phenyl signals.

Scheme 2

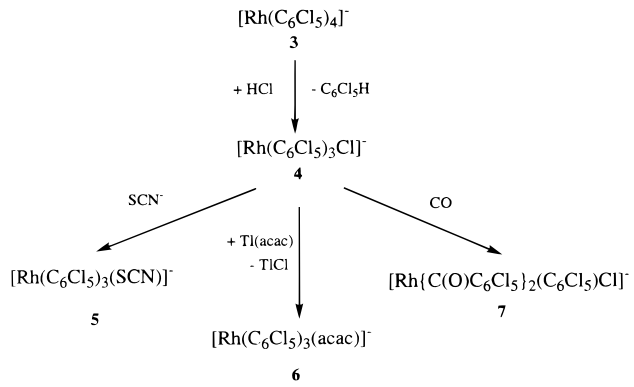

interactions are not maintained or a fluxional process probably involving breaking/formation of the Rh−Cl bonds takes place.

Electrochemistry of $[Rh(C_6Cl_5)_4]^{2-}$ and $[Rh(C_6Cl_5)_4]^-$. Complexes **1** and **3** have been studied by cyclic voltammetry. The dianion $[Rh(C_6Cl_5)_4]^{2-}$ (**1**) shows two successive irreversible oxidation waves at 0.22 and 1.26 V, together with two irreversible reduction waves at −1.39 and −1.12 V, respectively. An identical voltammogram is observed for the monoanion $[Rh(C_6Cl_5)_4]^-$ complex (**3**). The presence of two redox processes can be attributed to the existence of the rhodium atom in the oxidation states I, II, and III. Trying to prepare chemically the rhodium(I) anion $[Rh(C_6Cl_5)_4]^{3-}$, we treated complex **1b** with $[NBu_4][BH_4]$; they reacted, and evolution of H_2 took place, but from the reaction product it was not possible to isolate or identify any compound.

Synthesis and Reactivity of the Monoanion $[Rh(C_6Cl_5)_3Cl]^-$ (4). (Scheme 2) It seems convenient to mention that, working with the pentafluorophenyl ligand, we have described that the treatment of $[Rh(C_6F_5)_5]^{2-}$ with a methanolic solution of HCl (1:2 molar ratio) yields the dinuclear complex $[Rh_2(\mu\text{-Cl})_2(C_6F_5)_6]^{2-}$; similarly, the palladium and platinum dianions $[M(C_6X_5)_4]^{2-}$ (M = Pd, Pt; X = F, Cl) react with HCl, giving[17,22] the dinuclear complexes $[M_2(\mu\text{-Cl})_2(C_6X_5)_4]^{2-}$. Surprisingly, the reaction of complex **3** with HCl (molar ratio 1:2) does not give a dinuclear product; in this case the orange mononuclear complexes $[PBzPh_3][Rh(C_6Cl_5)_3Cl]$ (**4a**) and $[NBu_4][Rh(C_6Cl_5)_3Cl]$ (**4b**) are obtained. In the course of the reaction one Rh−C bond has been broken, but dimerization has not occurred. The IR spectra of **4a** and **4b** are in accord with the proposed formulation; they present the absorptions of the C_6Cl_5 ligands, as well as the ν(Rh−Cl) absorption at 285 cm^{-1}. The molecular structure of complex **4a**, established by X-ray crystallography, shows that the rhodium atom of the anion $[Rh(C_6Cl_5)_3Cl]^-$ is again six-coordinated (Scheme 1). The metal atom lies in a distorted-octahedral environment formed by three Rh−C σ bonds, one terminal Rh−Cl bond, and two Rh−Cl interactions from the *o*-chlorine atoms of two C_6Cl_5 groups. In solution, the ^{13}C NMR spectrum of **4b**, at room temperature, shows only one type of C_6Cl_5 group, while at −80 °C two different signals are observed for each of the *ipso*, *ortho*, *meta*, and *para* C atoms of the C_6Cl_5 rings. This behavior does not give a definitive indication about the presence or absence of the Rh−Cl interactions in solution, because in this complex, with or without the interactions, there should still be two different kinds of C_6Cl_5 groups: one *trans* and two *cis* to the terminal Cl atom.

The terminal chlorine ligand of complex **4** can be displaced by other anionic groups such as thiocyanate and acetylacetonate (acac). Prolonged treatment (18 h reflux and 3 days at room temperature) of a CH_2Cl_2 solution of the chloro complex **4a** with KSCN (molar ratio 1:1) gives a white solid (KCl) and a yellow solution. From the solution, after workup, the yellow complex $[PBzPh_3][Rh(C_6Cl_5)_3(SCN)]$ (**5**) is isolated. The IR spectrum, in the 1300 cm^{-1} region, is similar to that of complex **3**. The ν(CN) stretching vibration of the thiocyanate ligand is located at 2107 cm^{-1}; on the basis of the assignments suggested by Norbury[23] (ν(CN) for M−NCS at 2050−2100 cm^{-1} and M−SCN at 2085−2130 cm^{-1}), we proposed that the thiocyanate ligand is S- rather than N-bonded. In the ^{13}C NMR spectrum of **5** (Table 1), from the signals of the C_6Cl_5 groups, only the *ipso* and *ortho* C atoms can be identified; the other signals are overlapped with those of the phenyl rings of the $PBzPh_3$ cation. As occurs for the preceding complex, the spectrum shows, at room temperature, only one type of C_6Cl_5 group, while at −80 °C two different signals are observed for each of the *ipso* and *ortho* C

(22) Usón, R.; Fornies, J.; Martínez, F.; Tomás, M.; Reoyo, I. *Organometallics* **1983**, *2*, 1386. Usón, R.; Fornies, J.; Fandos, R.; Tomás, M. *J. Chem Soc., Dalton Trans.* **1980**, 888.

(23) Norbury, A. H. *Adv. Inorg. Chem. Radiochem.* **1975**, *17*, 231.

Downloaded by CARLI CONSORTIUM on June 30, 2009
Published on March 4, 1997 on http://pubs.acs.org | doi: 10.1021/om960663i

atoms of the C_6Cl_5 rings. The signal due to the C atom of the SCN ligand appears at δ 207.3 ppm.

Complex **4a** is also converted into the anionic mononuclear acetylacetonato (acac) derivative on treatment with thallium(I) acetylacetonate; thallium(I) chloride is precipitated and the new complex $[PBzPh_3][Rh(C_6Cl_5)_3(acac)]$ (**6**) can be readily isolated from the solution. The IR spectra of solid samples of **6** exhibit the strong absorptions of the acetylacetonate group, acting as a chelate,[24] at 1515 and 1585 cm^{-1}. The ^1H NMR spectrum of **6** shows acac as well as phenyl and benzyl resonances in the expected intensity ratio. The methyl groups of the acac ligand give only one signal at 1.6 ppm; therefore, in solution, the complex should be fluxional or it should present some molecular symmetry which makes both methyl groups equivalent.

Complex **4a** also reacts with CO, giving an acyl compound (Schemes 1 and 2). The insertion of CO into transition-metal−carbon bonds is a fundamental process in organometallic chemistry, both in stoichiometric and in catalytic reactions.[25] The reaction of dichloromethane solutions of complex **4a** with CO (20 °C, 1 atm) affords high yields of the stable diacyl complex $[PBzPh_3][Rh\{C(O)C_6Cl_5\}_2(C_6Cl_5)Cl]$ (**7**). The rhodium−acyl bonds give two intense IR absorptions at 1676 and 1636 cm^{-1}, *i.e.* in the region expected for rhodium(III) acyl complexes.[26] The presence of two acyl bands suggests that the two acyl groups are not equivalent. The IR spectrum also displays a sharp ν(Rh−Cl) absorption at 280 cm^{-1} together with bands due to the C_6Cl_5 groups. The mass spectrum (FAB negative) of **7** shows the parent peak of the anion $[Rh\{C(O)C_6Cl_5\}_2(C_6Cl_5)Cl]^-$ (*m*/*z* 941) and peaks at *m*/*z* 914 and 886 corresponding to the succesive losts of both CO groups. The ^{13}C NMR spectrum of **7** does not give any information about the complex, due to the low solubility of **7** in most solvents.

Molecular Structures of $[PBzPh_3]_2[Rh(C_6Cl_5)_4]$ (1a), $[PBzPh_3][Rh(C_6Cl_5)_4]\cdot CH_2Cl_2$ (3a·CH_2Cl_2), $[PBzPh_3][Rh(C_6Cl_5)_3Cl]\cdot{}^1/_2CH_2Cl_2\cdot{}^1/_2C_6H_{14}$ (4a·$^1/_2CH_2Cl_2{}^1/_2C_6H_{14}$), and $[PBzPh_3][Rh\{C(O)C_6Cl_5\}_2(C_6Cl_5)Cl]$ (7). As noted above, the crystal structures of **1a**, **3a**·CH_2Cl_2, **4a**·$^1/_2CH_2Cl_2\cdot{}^1/_2C_6H_{14}$, and **7** have been studied by single-crystal X-ray crystallography. The respective molecular structures of the anions—including conventional images of the displacement parameters—are presented in Figures 2−5, together with the atomic labeling schemes used. Selected bond distances and angles are collected in Tables 2−3. As is usual in rhodium(III) chemistry, all the molecular structures of the oxidized complexes **3a, 4a,** and **7** exhibit octahedral coordination around the metals, built up through normal bonding of the different ligands and *secondary bonding* interactions of the *o*-chlorine atoms of the pentachlorophenyl rings (see below). On the other side, the parent rhodium(II) complex **1a** shows a square-planar environment more closely related to the stereochemistry of rhodium(I) complexes.

The anionic complex of **1a** presents a crystallographically imposed C_2 symmetry, with the 2-fold axis bisecting two *trans*-disposed pentachlorophenyl rings. The metal center, bonded to four carbon atoms from the C_6Cl_5 ligands, is in a perfect square-planar arrangement with an interligand C(1)−Rh−C(9) angle of 90.4(5)°. The Rh−C bond distances are in the range 2.05(3)−2.09(2) Å and compare well with those found in the closely related square-planar rhodium(II) compound $[Rh(C_6Cl_5)_2\{P(OPh)_3\}_2]$ (2.080(4) Å).[8] The values of these distances are also similar to the Ir−C and Pt−C bond lengths observed in the isoelectronic and isostructural homoleptic iridium(II) and platinum(III) complexes $[Ir(C_6Cl_5)_4]^{2-}$ and $[Pt(C_6Cl_5)_4]^-$ (mean values 2.107(8) and 2.094(4) Å, respectively)[16,17b] and to that of the iridium(II) complex $[Ir(C_6Cl_5)_2(cod)]$ (2.073(5) Å).[15b] The two independent pentachlorophenyl groups are roughly planar, with the chlorine atoms slightly deviating from the mean planes (maximum deviation 0.135(5) Å, Cl(4)

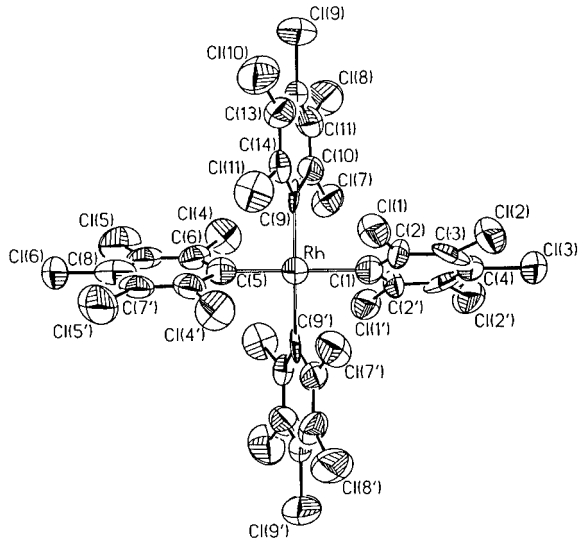

Figure 2. Molecular diagram of the anion of **1a**, $[Rh(C_6Cl_5)_4]^{2-}$. Selected bond lengths (Å) and angles (deg): Rh−C(1), 2.08(3); Rh−C(5), 2.05(3); Rh−C(9), 2.09(2); C−C, 1.33(3)-1.47(3); C−Cl, 1.68(2)-1.77(3); C(1)−Rh−C(9), 90.4(5); Rh−C(1)−C(2), 122.9(8); C(2)−C(1)−C(2′), 114(1); Rh−C(5)−C(6), 124.5(8); C(6)−C(5)−C(6′), 111(1); Rh−C(9)−C(10), 122(1); Rh−C(9)−C(14), 125(1); C(10)−C(9)−C(14), 113(2). Primed atoms are related to the unprimed ones by the symmetry transformation $-x, y, {}^1/_2 - z$.

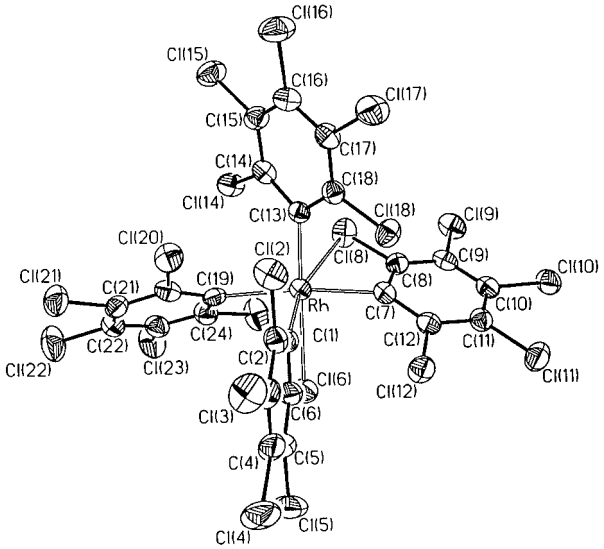

Figure 3. Molecular structure of the anion of **3a**, $[Rh(C_6Cl_5)_4]^-$.

Downloaded by CARLI CONSORTIUM on June 30, 2009
Published on March 4, 1997 on http://pubs.acs.org | doi: 10.1021/om960663i

(24) Bock, B.; Flatau, K.; Junge, H.; Kurh, M.; Musso, H. *Angew. Chem., Int. Ed. Engl.* **1971**, *10*, 225.
(25) Collman, J. P.; Hegedus, L. S.; Norton, J. R.; Finke, R. G. *Principles and Applications of Organotransition Metal Chemistry*; University Science Books: Mill Valley, CA, 1987.
(26) McGuiggan, M. F.; Doughty, D. H.; Pignolet, L. H. *J. Organomet. Chem.* **1980**, *185*, 241.

Table 2. Selected Bond Lengths (Å) and Angles (deg) for the Anions of 3a, $[Rh(C_6Cl_5)_4]^-$, and 4a, $[Rh(C_6Cl_5)_3Cl]^-$

	3a	4a		3a	4a
Rh−Cl(6)	2.6277(11)	2.656(4)	Rh−C(7)	2.106(4)	2.058(7)
Rh−Cl(8)	2.7521(11)	2.678(4)	Rh−C(13)	2.030(4)	2.019(6)
Rh−C(1)	2.005(4)	1.985(6)	Rh−C(19)/Cl(1)[a]	2.169(4)	2.419(3)
Cl(6)−Rh−Cl(8)	108.18(3)	95.73(8)	C(7)−Rh−C(19)/Cl(1)	162.67(14)	167.8(2)
Cl(6)−Rh−C(1)	67.46(11)	67.2(2)	C(13)−Rh−C(19)/Cl(1)	98.67(13)	97.1(2)
Cl(6)−Rh−C(7)	84.70(10)	78.5(2)	Rh−Cl(6)−C(6)	73.69(13)	72.8(2)
Cl(6)−Rh−C(13)	170.70(10)	167.7(2)	Rh−Cl(8)−C(8)	74.84(13)	74.3(2)
Cl(6)−Rh−C(19)/Cl(1)	83.67(10)	92.14(9)	Rh−C(1)−C(2)	140.3(3)	137.4(5)
Cl(8)−Rh−C(1)	164.09(10)	161.4(2)	Rh−C(1)−C(6)	105.4(3)	106.3(5)
Cl(8)−Rh−C(7)	63.95(10)	66.2(2)	Rh−C(7)−C(8)	107.3(3)	105.7(5)
Cl(8)−Rh−C(13)	79.77(10)	89.2(2)	Rh−C(7)−C(12)	138.1(3)	138.9(5)
Cl(8)−Rh−C(19)/Cl(1)	107.87(10)	107.45(8)	Rh−C(13)−C(14)	120.8(3)	120.3(5)
C(1)−Rh−C(7)	100.17(14)	101.7(3)	Rh−C(13)−C(18)	124.9(3)	125.7(5)
C(1)−Rh−C(13)	103.56(15)	106.1(3)	Rh−C(19)−C(20)	131.6(3)	
C(1)−Rh−C(19)/Cl(1)	87.17(14)	81.5(2)	Rh−C(19)−C(24)	114.3(3)	
C(7)−Rh−C(13)	94.86(14)	93.3(3)			

[a] Both structures **3a** and **4a** are closely related, with Cl(1) in **4a** approximately replacing C(19) in **3a**.

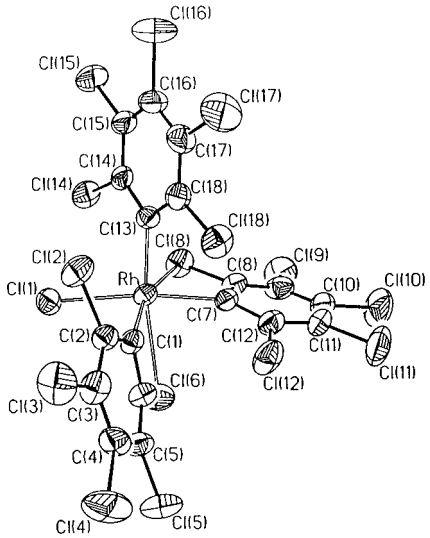

Figure 4. Molecular representation of the anion of **4a**, $[RhCl(C_6Cl_5)_3]^-$, including thermal displacement parameters and the numbering scheme used.

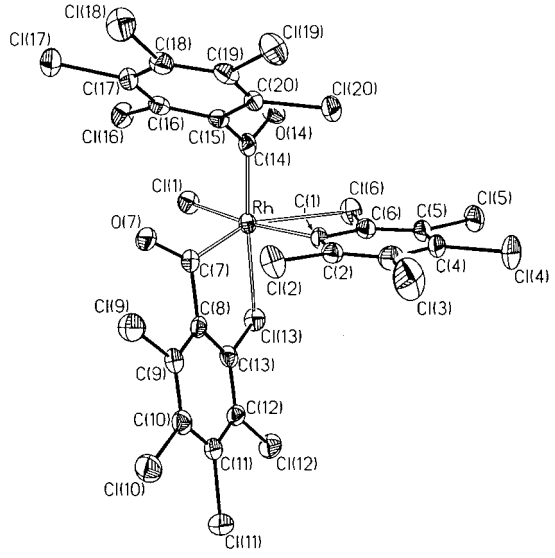

Figure 5. The diacyl anion of **7**, $[Rh\{C(O)C_6Cl_5\}_2(C_6Cl_5)Cl]^-$, together with the labeling system.

atom). The aryl rings are not perpendicular to the metal coordination plane and are all rotated in the same direction forming a chiral propeller-like structure for the

Table 3. Bond Lengths (Å) and Selected Angles (deg) for the Anion of 7, $[Rh\{C(O)C_6Cl_5\}_2(C_6Cl_5)Cl]^-$

Rh−Cl(1)	2.3927(9)	Rh−C(1)	2.044(3)
Rh−Cl(6)	2.8863(9)	Rh−C(7)	1.946(3)
Rh−Cl(13)	2.5859(9)	Rh−C(14)	1.953(3)
C(7)−O(7)	1.200(4)	C(14)−O(14)	1.208(4)
C(7)−C(8)	1.548(4)	C(14)−C(15)	1.521(4)
Cl(1)−Rh−Cl(6)	100.60(3)	Cl(6)−Rh−C(14)	93.33(10)
Cl(1)−Rh−Cl(13)	86.44(3)	Cl(13)−Rh−C(1)	90.97(9)
Cl(1)−Rh−C(1)	163.78(9)	Cl(13)−Rh−C(7)	82.20(10)
Cl(1)−Rh−C(7)	96.40(9)	Cl(13)−Rh−C(14)	174.74(10)
Cl(1)−Rh−C(14)	93.13(9)	C(1)−Rh−C(7)	99.11(12)
Cl(6)−Rh−Cl(13)	81.61(3)	C(1)−Rh−C(14)	87.99(13)
Cl(6)−Rh−C(1)	63.18(9)	C(7)−Rh−C(14)	103.06(14)
Cl(6)−Rh−C(7)	155.65(10)		
Rh−Cl(6)−C(6)	70.54(11)	Rh−Cl(13)−C(13)	94.03(11)
Rh−C(1)−C(2)	135.6(2)	Rh−C(1)−C(6)	109.6(2)
Rh−C(7)−O(7)	125.5(2)	Rh−C(14)−O(14)	115.0(2)
Rh−C(7)−C(8)	115.3(2)	Rh−C(14)−C(15)	127.4(2)
O(7)−C(7)−C(8)	118.8(3)	O(14)−C(14)−C(15)	117.6(3)

whole anionic complex (dihedral angles 69.4(4) and 70.7(5)°). This disposition of the C_6Cl_5 rings in **1a** closely resembles those observed in the structurally related $[Ir(C_6Cl_5)_4]^{2-}$ (dihedral angles 59.5(1) and 65.8(5)°)[16] and $[Pt(C_6Cl_5)_4]^-$ complexes (mean value 63.0°).[17b] These peculiar conformations of the phenyl rings are clearly due to steric forces. The adopted propeller-like structure reduces the interatomic repulsive interactions among the *o*-chlorines of the pentachlorophenyl rings (interatomic *o*-Cl···*o*-Cl distances 3.254−3.327(7) Å),[27] if compared with the two extreme situations in which the perhalophenyl rings could be disposed parallel (leading to the superimposition of the *o*-chlorine atoms) or perpendicular (*o*-Cl···*o*-Cl separations *ca.* 2.7 Å) to the metal coordination plane. Most probably the interconversion between the two enantiomers—differing in the conformational chirality of the anion—could be easily achieved by a synchronous rotation of the four C_6Cl_5 groups around the Rh−C_{ipso} bonds; an extended Hückel molecular orbital (EHT−MO) calculation on this fluxional movement for the anion of **1a,** assuming a simultaneous slight elongation of the Rh−C bond, shows that the process has a low activation barrier, less than 25 kcal/mol at the EHT level. For comparative purposes, it should be pointed

(27) (a) All the interatomic *o*-Cl···*o*-Cl separations in **1a** are shorter than twice the van der Waals radius of chlorine (3.50 Å).[27b] (b) Porterfield, W. W. *Inorganic Chemistry: A Unified Approach*; Addison-Wesley: Reading, MA, 1984; p 168.

Downloaded by CARLI CONSORTIUM on June 30, 2009
Published on March 4, 1997 on http://pubs.acs.org | doi: 10.1021/om960663i

Downloaded by CARLI CONSORTIUM on June 30, 2009
Published on March 4, 1997 on http://pubs.acs.org | doi: 10.1021/om960663i

out that the Rh···*o*-Cl separations in **1a** are in the range 3.403−3.429(6) Å, excluding any secondary bonding between the chlorines and the metal center (see below).

Although the stoichiometries of the anionic complexes of **1a** and **3a** are identical, the different oxidation states of the rhodium atoms dramatically affect the metal coordination sphere. The molecular structure of **3a** shows the rhodium atom located in a distorted-octahedral environment formed by four Rh−C σ bonds from the four C_6Cl_5 ligands and two Rh−Cl secondary bonds,[28] each involving one *o*-chlorine atom of two different pentachlorophenyl groups (Figure 3). Such a disposition of coordinated atoms (*OC*-6-32)[30] makes the anion chiral, although the presence of both enantiomers is observed in the crystal structure. Interestingly, this anionic structure of **3a** is isostructural with that of the isoelectronic platinum(IV) complex $[Pt(C_6Cl_5)_4]$.[31]

The structure of the anionic complex of **4a** is very similar to that described for $[Rh(C_6Cl_5)_4]^-$, with the unique minor change of the substitution of a κC-coordinated C_6Cl_5 group by a terminal chloride ligand. As in **3a**, the asymmetry of the metal-linked atoms makes the anion as a chiral moiety; the disposition of the coordinated ligands around the metal could be described with the *OC*-6-43 terminology[30] (Figure 4).

The distortion around the metals in the anionic complexes of **3a** and **4a** (and to lesser extent in **7**; see Table 3) arises fundamentally from the chelate coordination (κC,κ^2Cl) of two of the pentachlorophenyl ligands, which form strained four-membered metallacycles. This distortion of the metal environments can be visualized in the Cl−Rh−C bond angles, 67.46(11) and 63.95(10)° in **3a** and 67.2(2) and 66.2(2)° in **4a**, and is the origin of an asymmetric coordination of the phenyl rings, which are tilted to cause the *o*-chlorine atoms to approach the metal center. This tilting has also been observed in related pentafluorophenyl complexes[14c] and has been characterized in terms of the value of the interlinear angle between the Rh−C direction and the *pseudo*-2-fold axis defined through C_{ipso} and C_{para} (19.0(2) and 17.9(1)° in **3a** and 17.7(3) and 19.4(2)° in **4a**). The relative coplanarity of the phenyl rings of the chelate C_6Cl_5 groups with one of the planes of the ideal metal-coordination octahedra is noteworthy (10.9 and 15.1(1)° in **3a**, 10.8 and 12.8(2)° in **4a**, and 14.6(1)° in **7**); in clear contrast, the phenyl rings of the terminal C_6Cl_5 ligands are all significantly rotated with respect to the ideal metal coordination planes (43.2 and 54.8(1)° in **3a** and 51.5(2)° in **4a**).

The configurational asymmetry mentioned above for the anionic metal complexes is also markedly reflected in the rhodium-ligand bond distances. In **3a** all Rh−C lengths are statistically different, clearly affected by the *trans*-disposed ligands; thus, the two Rh−C bonds *trans* to chlorine atoms exhibit shorter and similar values (2.005(4) Å for C(1) and 2.030(4) Å for C(13)), with the shortest distance found for the carbon atom involved in the chelate coordination. The two remaining Rh−C distances, mutually *trans* disposed, are markedly longer, 2.106(4) and 2.169(4) Å, with the shortest again associated with the chelate C_6Cl_5 group. This pattern of Rh−C bond distances is analogous to that reported in the isoelectronic neutral platinum(IV) complex $[Pt(C_6Cl_5)_4]$ (Pt−C *trans* to Cl, 2.038(8) and 2.043(8) Å; Pt−C *trans* to C_6Cl_5, 2.119(7) and 2.139(7) Å).[31] The structural asymmetry of this anion (**3a**) found in the solid state contrasts with the presence of a unique signal for all aryl groups in the ^{13}C NMR spectrum, even at low temperature; a complex fluxional process should take place in solution involving most likely the breaking/formation of the weaker Rh−Cl secondary bonds.

In **4a**, the presence of three coordinated chlorine atoms reduces the dissimilarity of the Rh−C bond distances, 1.985(6)−2.058(7) Å. However, all Rh−C separations are different with the longest situated *trans* to the strongly bonded terminal chloride and the shortest associated with a chelate C_6Cl_5 ligand opposed to a secondary-bonded chlorine atom. The terminal Rh−Cl bond distance, 2.419(3) Å, is slightly longer than the usual Rh^{III}−Cl bond distances (mean value 2.374 Å),[32] presumably affected by the high *trans* influence of the perhaloaryl group.[14c,33]

The molecular structure of the anionic complex of **7** also maintains some similarities with those of **3a** and **4a**. The metal center exhibits a distorted-octahedral environment, completing the coordination sphere with three different ligands: a terminal chloride, two acyl COC_6Cl_5 ligands (one terminally κC-bonded and one κC,κ^2Cl chelate), and a C_6Cl_5 ligand linked to the metal through a Rh−C σ bond and through a secondary Rh−Cl bond (Figure 4). This distribution of ligands results in a chiral configuration with *OC*-6-45 descriptors. The terminal chloride atom displays a Rh−Cl length, 2.3927(9) Å, slightly shorter than that observed in **4a**, in the upper range of the hexacoordinated rhodium(III) complexes,[32] probably as a consequence of the *trans* influence of the pentachlorophenyl ring. On the opposite coordination site, the Rh−C(C_6Cl_5) bond distance (2.044(3) Å) is shorter than the distances reported for the related rhodium(II) complexes $[Rh(C_6Cl_5)_2\{P(OPh)_3\}_2]$ (2.080(4) Å)[8] or for the anionic form of **1a** (2.05(3)−2.09(2) Å) but compares well with some of the Rh−C distances found in **3a** (2.030(4) Å, C_6Cl_5 *trans* to secondary bonded chlorine) or in **4a** (2.058(7) Å, C_6Cl_5 ligand also *trans* to terminal chloride). Apparently, from the data accumulated in the present paper, the Rh−C(C_6Cl_5) bond distances seem to be rather sensitive to the influence of the *trans*-located ligand (range 1.985(6)−2.169(4) Å).

As far as we know, the anionic complex $[Rh\{C(O)C_6Cl_5\}_2(C_6Cl_5)Cl]^-$ represents the first mononuclear rhodium diacyl complex structurally characterized. Although the two Rh−C(acyl) bond distances are statistically equal (1.946 and 1.953(3) Å), both in the lower part of the range described for rhodium acyl complexes (1.93−2.13 Å),[32] the coordination mode of

(28) Although the *secondary-bonding* concept was originally proposed for intermolecular interactions showing distances much longer than normal single bonds and much shorter than the sum of the van der Waals radii (Alcock, N. W. *Adv. Inorg. Radiochem.* **1972**, *15*, 1), this intriguing concept has been also used to describe analogous intramolecular interactions.[29]

(29) Kulawiec, R. J.; Crabtree, R. H. *Coord. Chem. Rev.* **1990**, *99*, 89.

(30) Leigh, G. J. In *Nomenclature of Inorganic Compounds*; Blackwell Scientific: Oxford, U.K., 1991; p 159.

(31) Forniés, J.; Menjón, B.; Sanz-Carrillo, R. M.; Tomás, M.; Connelly, N. G.; Crossley, J. G.; Orpen, A. G. *J. Am. Chem. Soc.* **1995**, *11*, 4295.

(32) Orpen, A. G.; Brammer, L.; Allen, F. H.; Kennard, O.; Watson, D. G.; Taylor, R. in *International Tables for Crystallography;* Kluwer Academic: Dordrecht, The Netherlands, 1992; Vol. C, p 707.

(33) Appleton, T. G.; Clark, H. C.; Manzer, L. E. *Coord. Chem. Rev.* **1973**, *10*, 335.

each acyl group is rather different. In the terminally bonded $C(O)C_6Cl_5$ ligand, the plane defined by the ketonic group (around C(14)) is almost perpendicular to the pentachlorophenyl ring (dihedral angle 76.2(2)°). However, in the chelate acyl group both ideal planes, that of the ketonic carbon around C(7) and that of the C_6Cl_5 residue, present a dihedral angle substantially closer to coplanarity (31.4(3)°) to bring Cl(13) within coordination distance—secondary bond distance—of the rhodium atom. In both cases the metal-bonded ketonic carbons exhibit an sp^2 character, as is shown by the bond angles around them (*ca.* 120°). Interestingly, the Rh−C(acyl) bond distances determined in **7** compare well with some pentacoordinated mononuclear rhodium(III) complexes in which the acyl ligands occupy the apical position: for instance, in $[RhCl_2\{C(O)Pr\}(PPh_3)_2]$ (1.953(10) Å)[34] or in $[RhI\{C(O)Me\}(S_2PPh_2)(PPh_3)]$ (1.96(1) Å).[35]

Secondary Bonding of *o*-Chlorine Atoms. Probably the most intriguing feature of all the structures reported in this paper is the characterization of the interaction established between some *o*-chlorine atoms of the pentachlorophenyl rings and the central metal. This peculiar situation arises from the fact that, in some cases, the apparently nonbonded Rh···*o*-Cl distances are somewhat longer than the usual octahedral rhodium–terminal chloride distance (2.374 Å)[32] but show values well under the sum of the difficult-to-determine van der Walls radii of these two atoms, 3.38 Å (1.75 Å for Cl and 1.63 Å for Rh).[27b] Similar situations have also been reported for other pentachlorophenyl complexes of rhodium,[8] iridium,[15b] platinum,[31] and silver[36] and in the closely related pentafluorophenyl derivatives of rhodium[14a−c] and silver.[36] Other analogous short halogen−metal interactions have also been observed in related halocarbon transition-metal complexes.[29,37]

The concept of *secondary bonding* was proposed some years ago to account for this type of interaction[28] when it originates from *electronic bonding* effects rather than from intramolecular or intermolecular geometrical restraints (conformation of ligands, overcrowding of the coordination sphere, packing effects, etc.). Wulfsberg and co-workers have recently showed that the ^{35}Cl nuclear quadrupolar resonance (NQR) measurements can be alternatively used as a diagnostic tool for chlorocarbon secondary bonding recognition. They have correlated the ^{35}Cl NQR frequency differences between the signals of noncoordinated *o*-Cl (no metal interaction) and those of the coordinated *o*-Cl (potentially secondary bonded) as a function of the excess of the M−Cl distances (defined as the observed M−Cl distance minus the normal M−Cl single-bond distance) for several copper, silver, mercury, cobalt, zinc, and nickel 2,4,6-trichlorophenolate complexes.[38] Their results showed that a more restrictive and reliable criterion—compared to the van der Waals contact rule—to characterize the existence of metal−chlorine secondary bonding is associated with the elongation of the M−Cl separation relative to the normal M−Cl single-bond distance: excesses under 1.0 Å are indicative of the existence of metal−chlorine secondary bonding.[39] If applied to our structures, this criterion would establish a maximum Rh−Cl distance of 3.37 Å.

With the exception of the Rh···*o*-Cl distances observed in **1a** (3.403–3.429(6) Å), which are slightly over the limit of the van der Waals contact distance (3.38 Å) and also over that proposed by Wulfsberg (3.37 Å), all the remaining Rh–*o*-Cl(C_6Cl_5) distances (2.6277 and 2.7521(11) Å in **3a**, 2.656 and 2.678(4) Å in **4a**, and 2.5859 and 2.8863(9) Å in **7**) could be described as *secondary bonding* interactions and should be considered having a bonding nature, although the X-ray-detected distances notably exceed the normal Rh−Cl single-bond length. Several features support this statement.

In complexes **3a**, **4a**, and **7** these interactions seem to be the result of directed forces, *i.e.* bonds, rather than electrostatic or nondirectional van der Waals forces. In fact, the analysis of the metal coordination spheres reveals how these *o*-Cl atoms occupy stereochemically significant positions, that is, coordination sites of the distorted-octahedral environments (see Tables 2 and 3). Additionally, the pentachlorophenyl rings, when participating in secondary bonding, exhibit a clear unusual asymmetrical coordination (in terms of the interlinear angle $Rh-C_{ipso}$ *vs* $C_{ipso}-C_{para}$; see above) to favor the bonding between the *o*-chlorines and the rhodium atoms.

Trying to get a better understanding of the nature of the rhodium-to-*o*-chlorine interactions, we have carried out a theoretical study of the molecular orbital distribution using the extended Hückel approach,[40] starting from the crystallographic coordinates of **3a**, **4a**, and **7**. These calculations have shown the existence of a significant electron density between the metal center and the *o*-chlorine atoms, showing Mülliken populations of 0.235 and 0.188 e^- for **3a**, 0.212 and 0.224 e^- for **4a**, and 0.317 and 0.120 e^- for **7**. If we take as a point of reference the Mülliken population calculated, under the same approximations, for the terminal Rh−Cl single bonds, 0.333 e^- in **4a** and 0.357 e^- in **7**, it can be concluded that these interactions, although weaker than normal covalent bonds, should be considered strong enough to be maintained in solution or in reactivity processes involving weak donor solvents and/or ligands. This behavior has been reported for the closely related complex $[Pt(C_6Cl_5)_4]$, which maintains these secondary bonds even when dissolved in coordinating solvents such as acetone and acetonitrile.[31]

The metal−chlorine secondary bonds observed in our structures seem to imply the donation of electron density from the chlorine to the rhodium atom. We have

Downloaded by CARLI CONSORTIUM on June 30, 2009
Published on March 4, 1997 on http://pubs.acs.org | doi: 10.1021/om960663i

(34) Shie, J.-Y.; Lin, Y.-C.; Wang, Y. *J. Organomet. Chem.* **1989**, *371*, 383.
(35) Cabeza, J.; Riera, V.; Villa-García, M. A.; Ouahab, L.; Triki, S. *J. Organomet. Chem.* **1992**, *441*, 323.
(36) Usón, R.; Forniés, J.; Tomás, M. *J. Organomet. Chem.* **1988**, *358*, 525.
(37) Harrison, R.; Arif, A. M.; Wulfsberg, G.; Lang, R.; Ju, T.; Kiss, G.; Hoff, C. D.; Richmond, T. G. *J. Chem. Soc., Chem. Commun.* **1992**, 1374. Lahuerta, P.; Peris, E.; Ubeda. M. A.; García-Granda, S.; Gómez-Beltrán, F.; Díaz, M. R. *J. Organomet. Chem.* **1993**, *455*, C10. García-Bernabé, A.; Lahuerta, P.; Ubeda, M. A.; García-Granda, S.; Pertierra, P. *Inorg. Chim. Acta* **1995**, *229*, 203. Van Seggen, D. M.; Hurlburt, P. K.; Anderson, O. P.; Strauss, S. H. *Inorg. Chem.* **1995**, *34*, 3453 and references therein.
(38) Meyer, R.; Gagliardi, J., Jr.; Wulfsberg, G. *J. Mol. Struct.* **1983**, *111*, 311. Wulfsberg, G.; Yanisch, J.; Meyer, R.; Bowers, J.; Essig, M. *Inorg. Chem.* **1984**, *23*, 715. Wulfsberg, G.; Jackson, D.; Ilsley, W.; Dou, S.; Weiss, A; Gagliardi, J., Jr. *Z. Naturforsch.* **1992**, *47A*, 75.
(39) Richardson, M. F.; Wulfsberg, G.; Marlow, R.; Zaghonni, S.; McCorkle, D.; Shadid, K.; Gagliardi, J., Jr.; Farris, B. *Inorg. Chem.* **1993**, *32*, 1913.
(40) Mealli, C.; Proserpio, D. M. *J. Chem. Educ.* **1990**, *67*, 39.

checked this proposal by comparing the calculated charges at the secondary-bonded Cl(6) and Cl(8) atoms in the real structure **4a** (0.147 and 0.145), with those estimated for a hypothetical identical structure with the Rh−Cl overlap populations constrained to be zero, *i.e.*, with no secondary bonding (−0.111 and −0.112). From these data, it is clear that the formation of the secondary bonds implies an electron donation to the metal center that reduces the formal negative charge at these chlorine atoms. A further question arises: What kind of atomic orbital does this electron density come from?

The lone pairs of the chlorine atoms suitable to form a secondary bond with the metal can be envisaged to lie between two extreme representations: (i) a more stable sp hybrid and two pure *p* orbitals at higher energy and (ii) three equivalent sp^3 orbitals. From a structural point of view we have considered the Rh−Cl−C bond angles, as these parameters could differentiate both models.[41] The values observed (73.7(1) and 74.8(1)° in **3a,** 72.8(2) and 74.3(2)° in **4a**, and 70.5(1) and 94.0(1)° in **7**) suggest model i to be more reasonable, as these parameters are closer to the ideal value of 90°. Additionally, model i would leave the second p pure orbital in the appropriate disposition to interact with the aromatic system of the phenyl ring. Also in accord with this proposal, the C−Cl bond distances observed for the secondary-bonded chlorine atoms (1.744 and 1.750(4) Å in **3a**, 1.754(7) Å in **4a**, and 1.749(4) and 1.734(4) Å in **7**) are almost unaffected (mean uncoordinated C−Cl distances 1.730(2) Å in **3a**, 1.728(2) Å in **4a**, and 1.724(2) Å in **7**) upon coordination to the metal, also supporting the notion that the C−Cl and Rh−Cl bonds involve different and orthogonal atomic orbitals: hybrid sp for C−Cl and pure p for Rh−Cl.

Concluding Remarks

With the preparation of $[Rh(C_6Cl_5)_4]^{2-}$ we have obtained further evidence of the potential of the C_6Cl_5 group to stabilize anomalous oxidation states, rhodium(II) in our case. This species is oxidized by chlorine or iodine, giving the stoichiometric analogous rhodium(III) anion $[Rh(C_6Cl_5)_4]^-$ (**3**). Interestingly, the latter complex **3** reacts with HCl in an unusual way to yield the mononuclear $[RhCl(C_6Cl_5)_3]^-$ complex **4**, in contrast with the usual dimerization through bridging chloride ligands found for related complexes. The terminal chlorine ligand in complex **4** could be substituted by a variety of anionic groups, while the reaction with carbon monoxide renders the diacyl complex **7** through the insertion of CO into the Rh−C bonds.

The structural analyses carried out for **1a**, **3a**, **4a**, and **7** have shown the capacity of the pentachlorophenyl groups to act as chelate ligands, through the formation of secondary bonds between the *o*-chlorine substituents of the phenyl rings and the metal center. From the structural parameters and the theoretical calculations performed, we can conclude that this secondary bonding exhibits characteristics analogous to those of the normal covalent bonds and implies the donation of electron density from *p* atomic orbitals of the chlorine to the rhodium atom. These types of interactions are of reasonable strength and should be kept in mind in the design or in the interpretation of reactivity processes involving *o*-haloaryl groups or related ligands.

Experimental Section

General Data. C, H, and N analyses, conductance determinations, and IR spectra (in CH_2Cl_2 solution or Nujol suspension between polyethylene sheets) were performed as described elsewhere[8]. Mass spectra were measured in a VG Autospec double-focusing mass spectrometer operating in the negative mode: ions were produced with the standard Cs^+ gun at ca. 30 kV; 3-nitrobenzyl alcohol (NBA) was used as matrix; high-resolution FAB spectra are in accordance with the simulated isotopic pattern distribution. Cyclic voltammetric experiments were performed by employing an EG&G PARC Model 273 potentiostat. A three-electrode system was used, which consists of a platinum-disk working electrode, a platinum-wire auxiliary electrode, and a saturated calomel reference electrode. The measurements were carried out in CH_2Cl_2 solutions with 0.1 M Bu_4NPF_6 as supporting electrolyte. Under the present experimental conditions the ferrocenium/ferrocene couple was located at 0.47 V. EPR data were measured with a Varian E-112 spectrometer working in the X-band. The powdered polycrystalline samples were introduced in a standard EPR quartz tube (707-SQ from Wilmad) and their spectra were taken at room temperature. The magnetic field was measured with an NMR gauss meter (Bruker ER035M), and the diphenylpicrylhydrazyl (DPPH) resonance signal ($g = 2.0037 \pm 0.0002$) was used for determining the microwave frequencies. The starting rhodium(III) compound $[RhCl_3(tht)_3]$ was prepared as described in the literature.[42] LiC_6Cl_5 was obtained as described in ref 43 and was directly used without further isolation. Solutions of chlorine were prepared by bubbling a stream of the dry gas through CCl_4 and were titrated by standard redox methods[44] before use. Diethyl ether, THF, CH_2Cl_2, and hexane were distilled under nitrogen from the appropriate drying agents.

$Q_2[Rh(C_6Cl_5)_4]$ (Q = $PBzPh_3$ (1a), NBu_4 (1b)). Solid $[RhCl_3(tht)_3]$ (0.500 g, 1.05 mmol) was added to a diethyl ether solution (30 mL) of LiC_6Cl_5 (10.53 mmol) at −50 °C. The mixture was warmed slowly to room temperature, hydrolyzed with aqueous diethyl ether, and then evaporated to dryness. The residue was treated with methanol (20 mL) and the solution filtered; to this solution was added $PBzPh_3Cl$ (0.817 g, 2.1 mmol) or NBu_4Br (0.677 g, 2.1 mmol), yielding yellow solids which were filtered, washed with methanol, and dried in vacuo. Yield: **1a**, 65%; **1b**, 52%. Data for **1a** are as follows. Anal. Calcd for $C_{74}H_{44}Cl_{20}P_2Rh$: C, 49.18; H, 2.45. Found: C, 49.22; H, 2.53. IR (Nujol; $\nu(C_6Cl_5)$, cm^{-1}): 1314, 1294 (sh) 1275, 665. MS (FAB; *m/e* (%)): 1452 (20) $[Rh(C_6Cl_5)_4 \cdot PBzPh_3 - H]$, 1100 (100) $[M^-, Rh(C_6Cl_5)_4]$, 850 (31) $[Rh(C_6Cl_5)_3]$, 601 (78) $[Rh(C_6Cl_5)_2]$. Conductivity (in 4.3×10^{-4} M acetone solution): 185 $\Omega^{-1}cm^2\ mol^{-1}$. Data for **1b** are as follows. Anal. Calcd for $C_{56}H_{72}Cl_{20}N_2Rh$: C, 42.43; H, 4.58; N, 1.77. Found: C, 42.30; H, 4.63, N, 1.72. IR (Nujol, cm^{-1}): $\nu(C_6Cl_5)$ 1312, 1298 (sh), 1283, 812 (X-sensitive), 670, 583 [ν(Rh−C)]. MS (FAB; *m/e* (%)): 1100 (100) $[M^-, Rh(C_6Cl_5)_4]$, 601 (53) $[Rh(C_6Cl_5)_2]$. Conductivity (in 5.9×10^{-4} M acetone solution): 181 $\Omega^{-1}cm^2\ mol^{-1}$.

$[PBzPh_3][Rh(C_6Cl_5)_2(CO)_2]$ (2). A CH_2Cl_2 suspension of **1a** (200 mg, 0.111 mmol) was treated with CO (1 atm, room temperature) for 4 h. After concentration to about 1 mL, the microcrystalline yellow solid was precipitated by addition of hexane. Yield: 43%. Anal. Calcd for $C_{39}H_{22}Cl_{10}O_2PRh$: C, 46.33; H, 2.19. Found: C, 46.60; H, 2.31. IR (CH_2Cl_2; ν(CO), cm^{-1}): 2041, 1971. IR (Nujol; cm^{-1}): ν(CO) 2035, 1965; $\nu(C_6$-

(41) Burk, M. J.; Crabtree, R. H.; Holt, E. M. *J. Organomet. Chem.* **1988**, *341*, 495.

(42) Allen, E. A.; Wilkinson, G. *J. Chem. Soc., Dalton Trans.* **1972**, 613.

(43) Rausch, M. D.; Moser, G. A.; Meade, C. F. *J. Organomet. Chem.* **1973**, *51*, 1.

(44) Bermejo, F. *Tratado de Química Analítica*, 6th ed.; Editorial Dossat: Madrid, 1981; p 813.

Downloaded by CARLI CONSORTIUM on June 30, 2009
Published on March 4, 1997 on http://pubs.acs.org | doi: 10.1021/om960663i

Downloaded by CARLI CONSORTIUM on June 30, 2009
Published on March 4, 1997 on http://pubs.acs.org | doi: 10.1021/om960663i

Cl_5) 1324, 1308, 1282. MS (FAB; *m/e* (%)): 656 (100) [$Rh(C_6Cl_5)_2(CO)_2$], 601 (85) [$Rh(C_6Cl_5)_2$]. Conductivity (in 5.1×10^{-4} M acetone solution): 103 $\Omega^{-1}cm^2$ mol^{-1}.

Q[Rh(C_6Cl_5)$_4$] (Q = PBzPh$_3$ (3a), NBu$_4$ (3b)). (a) Oxidation of 1 with Chlorine. To a solution of **1a** (0.150 g, 0.083 mmol) in acetone (15 mL) was added chlorine (0.108 mmol) dissolved in CCl_4, and the mixture was stirred for 1 h. The solvent was removed; the residue was washed with water to eliminate the [$PBzPh_3$]Cl formed and dissolved in CH_2Cl_2 and the solution treated with anhydrous $MgSO_4$. Filtration of the $MgSO_4$, partial evaporation of the CH_2Cl_2, and addition of hexane or pentane gave **3a** as a yellow solid. Yield: 71%. The synthesis of [NBu_4][$Rh(C_6Cl_5)_4$] (**3b**) was carried out as reported for **3a**, starting with [NBu_4]$_2$[$Rh(C_6Cl_5)_4$] (0.200 g, 0.126 mmol) and chlorine (0.130 mmol): orange; 75% yield.

(b) Oxidation of 1 with Iodine. A CH_2Cl_2 (15 mL) suspension of **1a** (0.200 g, 0.11 mmol) was treated with iodine (0.070 g, 0.275 mmol). The solid dissolved, and the solution turned brown; after 2 h of stirring the solvent was pumped off. The residue was washed with water (5 mL) and then dissolved in CH_2Cl_2; this solution was treated with $MgSO_4$ and filtered. Evaporation of the filtrate to *ca.* 1 mL and addition of hexane led to a brown solid mixture of complex **3a** and [$PBzPh_3$][I_3]. From the mixture, both complexes were separated by extracting **3a** with diethyl ether, a solvent in which it is slightly soluble. Data for **3a** are as follows. Anal. Calcd for $C_{49}H_{22}Cl_{20}PRh$: C, 40.48; H, 1.52. Found: C, 40.27; H, 1.40. IR (Nujol; cm^{-1}): $\nu(C_6Cl_5)$ 1340, 1325, 1315, 1280, 670. MS (FAB; *m/e* (%)): 1100 (100) [M^-, $Rh(C_6Cl_5)_4$], 601 (28) [$Rh(C_6Cl_5)_2$]. Conductivity (in 5.0×10^{-4} M acetone solution): 96 $\Omega^{-1}cm^2$ mol^{-1}. Data for **3b** are as follows. Anal. Calcd for $C_{40}H_{36}Cl_{20}NRh$: C, 35.78; H, 2.70; N, 1.04. Found: C, 35.85; H, 2.63; N, 1.02. IR (Nujol; cm^{-1}): $\nu(C_6Cl_5)$ 1336, 1325, 1306, 1283, 820 (X-sensitive), 670, 617 [ν(Rh−C)].

Q[Rh(C_6Cl_5)$_3$Cl] (Q = PBzPh$_3$ (4a), or NBu$_4$ (4b)). A solution of **3a** (0.150 g, 0.103 mmol) in CH_2Cl_2 (15 mL) was treated with a 0.46 M methanol solution of HCl (0.46 mL, 0.212 mmol) and stirred for 1 h at room temperature. After concentration to about 1 mL, a microcrystalline orange solid was precipitated by addition of *n*-hexane, filtered off, and washed with hexane. Yield: 80%. The synthesis of [NBu_4][$Rh(C_6Cl_5)_3Cl$] (**4b**) was carried out as reported for **4a**, starting with [NBu_4][$Rh(C_6Cl_5)_4$] (**3b**; 0.200 g, 0.149 mmol) and HCl (0.30 mmol): orange; 86% yield. Data for **4a** are as follows. Anal. Calcd for $C_{43}H_{22}Cl_{16}PRh$: C, 41.66; H, 1.79. Found: C, 41.64; H, 1.95. IR (Nujol; cm^{-1}): ν(Rh−Cl) 285; $\nu(C_6Cl_5)$ 1350, 1328, 1315, 1285, 685. MS (FAB; *m/e* (%)): 887 (100) [M^-, $Rh(C_6Cl_5)_3Cl$], 601 (90) [$Rh(C_6Cl_5)_2$]. Conductivity (in 6.0×10^{-4} M acetone solution): 87 $\Omega^{-1}cm^2$ mol^{-1}. Data for **4b** are as follows. Anal. Calcd for $C_{34}H_{36}Cl_{16}NRh$: C, 36.18; H, 3.21; N, 1.24. Found: C, 36.34; H, 3.31; N, 1.21. IR (Nujol; cm^{-1}): ν(Rh−Cl) 285; $\nu(C_6Cl_5)$ 1341, 1325, 1311, 1284, 828 (X-sensitive), 685, 615 [ν(Rh−C)].

[PBzPh$_3$][Rh(C_6Cl_5)$_3$(SCN)] (5). A solution of **4a** (0.090 g, 0.073 mmol) and KSCN (0.007 g, 0.073 mmol) in CH_2Cl_2 (15 mL) was stirred at reflux temperature for 18 h and then at room temperature for 3 days. The white precipitate (KCl) was filtered. Partial evaporation of the filtrate and addition of hexane (10 mL) resulted in crystallization of **5** as an orange solid (74 mg, 81% yield). Anal. Calcd for $C_{44}H_{22}Cl_{15}NPRhS$: C, 41.86; H, 1.76; N, 1.11; S, 2.54. Found: C, 42.09; H, 1.82; N, 1.08; S, 2.43. IR (Nujol; cm^{-1}): ν(CN) 2107; $\nu(C_6Cl_5)$ 1340, 1329, 1313, 1286, 686. MS (FAB; *m/e* (%)): 907 (100) [M^-, $Rh(C_6Cl_5)_3(SCN)$], 601 (95) [$Rh(C_6Cl_5)_2$]. Conductivity (in 2.2×10^{-4} M acetone solution): 95 $\Omega^{-1}cm^2$ mol^{-1}.

[PBzPh$_3$][Rh(C_6Cl_5)$_3$(acac)] (6). To a CH_2Cl_2 solution of **4a** (0.100 g, 0.080 mmol) was added thallium(I) acetylacetonate (0.026 g, 0.08 mmol). After it was stirred for 30 min, the mixture gave an orange solution and a white solid (TlCl), which was eliminated by filtration through Kieselguhr. Evaporation of the solution under vacuum to 1 mL and addition of hexane afforded **6**, which was separated by filtration, washed with hexane and methanol, and vacuum-dried. Yield: 0.093 g, 89%. Anal. Calcd for $C_{48}H_{29}Cl_{15}O_2PRh$: C, 44.23; H, 2.24. Found: C, 44.40; H, 2.30. IR (Nujol; cm^{-1}): acac 1585, 1515; $\nu(C_6Cl_5)$ 1335, 1323, 1285, 615. Conductivity (in 4.5×10^{-4} M acetone solution): 98 $\Omega^{-1}cm^2$ mol^{-1}. ^1H NMR (20 °C, $CDCl_3$, δ): 7.8−6.8 (20H, phenyl), 4.8 (2H, >CH_2, $PBzPh_3^+$, ^2J(H−P) = 13.9 Hz), 5.28 (1H, >CH, acac), 1.6 (6H, −CH_3, acac).

[PBzPh$_3$][Rh{C(O)C_6Cl_5}$_2$(C_6Cl_5)Cl] (7). Through a CH_2Cl_2 solution of **4a** (0.100 g, 0.080 mmol), CO (1 atm, room temperature) was bubbled for 1 h; complex **7** was formed as a yellow solid which was separated by filtration and vacuum-dried. Yield: 82%. Anal. Calcd for $C_{45}H_{22}Cl_{16}O_2PRh$: C, 41.71; H, 1.71. Found: C, 41.53; H, 1.65. IR (Nujol; cm^{-1}): ν(CO) 1676, 1636; ν(Rh−Cl) 280; $\nu(C_6Cl_5)$ 1340, 1331, 1317, 1312. MS (FAB; *m/e* (%)): 942 (35) [$Rh(C_6Cl_5)_3Cl(CO)_2$], 914 (10) [$Rh(C_6Cl_5)_3Cl(CO)$], 886 (78) [$Rh(C_6Cl_5)_3Cl$], 601 (100) [$Rh(C_6Cl_5)_2$].

X-ray Structural Analyses of the Complexes [PBzPh$_3$]$_2$[Rh(C_6Cl_5)$_4$] (1a), [PBzPh$_3$][Rh(C_6Cl_5)$_4$] (3a), [PBzPh$_3$][Rh(C_6Cl_5)$_3$Cl] (4a), and [PBzPh$_3$][Rh{C(O)C_6Cl_5}$_2$(C_6Cl_5)Cl] (7). A summary of crystal data and refinement parameters is reported in Table 4. Data were collected on a Siemens AED with niobium-filtered MoKα radiation (**1a**) or on Siemens-Stoe AED-2 (**3a**, **7**) and Pillips PW1100 diffractometers (**4a**) with graphite-monochromated MoKα radiation, using in all cases the $\omega/2\theta$ scan method. A set of standard reflections were monitored every 100 measurements (**1a**, **4a**) or every 55 min of measurement time (**3a**, **7**) throughout data collection; no important variations were observed. All data were corrected for Lorentz and polarization effects and for absorption using a semiempirical method[45] (transmission factors are listed in Table 4). All structures were solved by Patterson and Fourier techniques and refined by full-matrix least squares on F (SHELX-76)[46] (**1a**, **3a**) or F^2 (SHELXL-93)[47] (**4a, 7**). Atomic scattering factors, corrected for anomalous dispersion, were used as implemented in the refinement program[47] or taken from ref 48.

Data for 1a. Crystals suitable for the X-ray diffraction study were obtained by slow diffusion of diethyl ether through an acetone solution of **1a**. A yellow prismatic block was indexed to monoclinic symmetry. Anisotropic displacement parameters were used in the last cycles of refinement for all non-hydrogen atoms, except for the carbon atoms of the phenyl rings of the cation. The hydrogen atoms were introduced in calculated positions (C−H = 0.96 Å) and refined riding on the corresponding carbon atoms. The weighting scheme used in the final steps of refinement was $w = 1/\sigma^2(F_o)$. The largest peak in the final difference map is 0.47 e $Å^{-3}$.

Data for 3a·CH$_2$Cl$_2$. Crystals suitable for the X-ray diffraction study were obtained by slow diffusion of hexane through a CH_2Cl_2 solution of **3a**. An orange crystalline needle was mounted on the top of a glass fiber, and a set of randomly searched reflections were indexed to monoclinic symmetry. After refinement of all non-hydrogen atoms with anisotropic displacement parameters, the hydrogen atoms were located in a difference Fourier map and introduced in the refinement riding on the corresponding carbon atoms. A dichloromethane solvate molecule was found in the residual map having one chlorine atom disordered; this atom was included in two different positions with complementary refined occupancy factors (0.57(7) and 0.43(7)). The hydrogen atoms for this solvent molecule were not included in the model. The weighting scheme used was $w = 1/(\sigma^2(F_o) + 0.000194F^2)$. Residual peaks in the final difference map were 0.86 and −0.50 e $Å^{-3}$.

(45) North, A. C. T.; Phillips, D. C.; Mathews, F. S. *Acta Crystallogr.* **1968**, *A24*, 351.
(46) Sheldrick, G. M. SHELX-76. Program for Crystal Structure Determination; University of Cambridge, Cambridge, U.K., 1976.
(47) Sheldrick, G. M. SHELXL-93; University of Göttingen, Göttingen, Germany, 1993.
(48) *International Tables for X-Ray Crystallography*; Kynoch Press: Birmingham, U.K., 1974; Vol. 4.

Table 4. Crystallographic Data for the Compounds 1a, 3a·CH_2Cl_2, 4a·$^1/_2CH_2Cl_2$·$^1/_2C_6H_{14}$, and 7

compd	$[PBzPh_3]_2[Rh(C_6Cl_5)_4]$ (**1a**)	$[PBzPh_3][Rh(C_6Cl_5)_4]$·CH_2Cl_2 (**3a**·CH_2Cl_2)	$[PBzPh_3][Rh(C_6Cl_5)_3Cl]$·$^1/_2CH_2Cl_2$·$^1/_2C_6H_{14}$ (**4a**·$^1/_2CH_2Cl_2$·$^1/_2C_6H_{14}$)	$[PBzPh_3][Rh(C(O)C_6Cl_5)_2(C_6Cl_5)Cl]$ (**7**)
cryst color, habit	yellow, prismatic block	orange, needle	orange, prismatic block	yellow-orange, pyramidal block
cryst size, mm	0.10 × 0.15 × 0.23	0.22 × 0.23 × 0.72	0.15 × 0.23 × 0.32	0.14 × 0.17 × 0.44
chem formula	$C_{74}H_{44}Cl_{20}P_2Rh$	$C_{49}H_{22}Cl_{20}PRh$·CH_2Cl_2	$C_{43}H_{22}Cl_{16}PRh$·$^1/_2CH_2Cl_2$·$^1/_2C_6H_{14}$	$C_{45}H_{22}Cl_{16}O_2PRh$
fw	1807.08	1538.59	1324.23	1295.71
cryst syst	monoclinic	monoclinic	monoclinic	monoclinic
space group	*C*2/*c* (No. 15)	$P2_1/n$ (No. 14)	*C*2/*c* (No. 15)	*Pn* (No. 7)
a, Å	19.094(7)	10.137(1)	32.34(3)	12.147(2)
b, Å	17.063(7)	26.642(2)	11.75(2)	11.982(2)
c, Å	23.623(8)	21.108(2)	29.38(4)	17.326(3)
β, deg	104.05(2)	94.53(1)	103.90(11)	105.955(12)
V, Å^3	7466(5)	5682.8(9)	10843(25)	2424.6(6)
Z	4	4	8	2
ρ(calcd), g cm^{-3}	1.608	1.798	1.622	1.775
μ, mm^{-1}	1.032	1.401	1.216	1.307
diffractometer	Siemens AED	Stoe-Siemens AED-2	Phillips PW1100	Stoe-Siemens AED-2
θ range data collecn, deg	3.0−23.0	1.5−25.0	3.0−27.0	2.09−25.09
temp, K	293(2)	233.0(2)	293(2)	173.0(2)
index ranges	$-19 \le h \le 19$, $0 \le k \le 18$, $0 \le l \le 21$	$0 \le h \le 12$, $0 \le k \le 32$, $-25 \le l \le 24$	$-41 \le h \le 39$, $0 \le k \le 15$, $0 \le l \le 37$	$-14 \le h \le 0$, $-14 \le k \le 0$, $-20 \le l \le 0$; $0 \le h \le 14$, $0 \le k \le 14$, $0 \le l \le 20$
no. of collected rflns	5555	11 816	12 596	10 222
no. of unique rflns	5185 (R_{int} = 0.0238)	9973 (R_{int} = 0.0191)	7536 (R_{int} = 0.0178)	8600 (R_{int} = 0.0172)
abs cor method	not applied	ψ-scan (12 ref)	ψ-scan (3 ref)	ψ-scan (18 ref)
min, max transm factors		0.430, 0.458	0.554, 0.690	0.659, 0.700
no. of data/restraints/params	1584/0/322	7909/0/678	7526/17/593	8597/0/586
$R(F)$ ($F^2 > 2\sigma(F^2)$)[a]	0.0587	0.0370	0.0524 (7524 obs ref)	0.0233 (8282 obs ref)
$R_w(F)$ ($F^2 > 2\sigma(F^2)$)[b]	0.0444	0.0374		
$R_w(F^2)$ (all data)[c]			0.1733	0.0553
S	1.183[d]	1.532[d]	1.146[e]	1.044[e]

[a] $R(F) = \sum||F_o| - |F_c||/\sum|F_o|$. [b] $R_w(F) = \sum(w^{1/2}||F_o| - |F_c||)/\sum(w^{1/2}|F_o|)$. [c] $R_w(F^2) = (\sum[w(F_o^2 - F_c^2)^2]/\sum[w(F_o^2)^2])^{1/2}$. [d] $S = [\sum[w(F_o - F_c)^2]/(n - p)]^{1/2}$. [e] $S = [\sum[w(F_o^2 - F_c^2)^2]/(n - p)]^{1/2}$; n = number of reflections used in refinement, p = number of parameters.

Data for 4a·$^1/_2CH_2Cl_2$·$^1/_2C_6H_{14}$. Crystals suitable for the X-ray diffraction study were formed at the interface between a dilute CH_2Cl_2 solution of the complex and pure hexane. An orange prismatic block was selected and the randomly obtained diffraction pattern indexed to monoclinic symmetry. Anisotropic displacement parameters were used in the last cycles of refinement for all non-hydrogen atoms, except those of the disordered solvent molecules (dichloromethane and hexane). The hydrogen atoms of the cation were introduced in calculated positions and refined riding on the corresponding carbon atoms. The solvent molecules were modeled on the base of two independent half-molecules of dichloromethane and hexane. The dichloromethane molecule was observed disordered over two positions, and common fixed occupancy (0.25) and thermal parameters were used for both moieties. The hexane solvent half-molecule was localized close to a crystallographic 2-fold axis; again two groups of atoms (fixed occupancy factors) were necessary to account for the residual electronic density. Geometric restrictions (DFIX command)[47] were neccessary for both disordered molecules. The weighting scheme used was $w^{-1} = [\sigma^2(F_o^2) + (xP)^2 + yP]$ ($P = (F_o^2 + 2F_c^2)/3$) with $x = 0.0244$ and $y = 0.0638$. Residual peaks in the final difference map were 1.585 and −1.069 e Å^{-3}, near the disordered dichloromethane molecule.

Data for 7. Due to its low solubility, single crystals of **7** were grown by slow diffusion of methanol, at room temperature, into a hot dichloromethane solution of **4a** saturated with carbon monoxide. A yellow-orange pyramidal crystal was selected and the randomly obtained diffraction pattern indexed to monoclinic symmetry. This structure was solved using SIR92.[49] Anisotropic displacement parameters were used in the last cycles of refinement for all non-hydrogen atoms. The hydrogen atoms of the cation were found in the difference Fourier map and refined with a common displacement parameter riding on the corresponding carbon atoms. The weighting scheme used was $w^{-1} = [\sigma^2(F_o^2) + (xP)^2 + yP]$ ($P = (F_o^2 + 2F_c^2)/3$) with $x = 0.0234$ and $y = 0.8765$. The absolute structure (*Pn* space group) was checked by refining the Flack parameter (−0.04(2)).[50] Residual peaks in the final difference map were 0.327 and −0.271 e Å^{-3}.

Appendix

Calculations of the extended Hückel type were carried out using a modified version of the Wolfsberg−Helmholtz formula.[51] The geometrical parameters of the compounds investigated were as close as possible to the reported crystal structures. Atomic parameters used were those of Alvarez,[52] and the calculations were made with the program CACAO.[40]

Acknowledgment. We thank Prof. Dr. P. Alonso for the measurement of the EPR spectra and the DGICYT (Dirección General de Investigación Científica y Técnica) for financial support (Project No. PB92-0032).

Supporting Information Available: Tables of all bond lengths and angles, isotropic and anisotropic displacement parameters, all atomic coordinates, least-squares planes, and intramolecular contacts for **1a**, **3a**, **4a**, and **7** (61 pages). Ordering information is given on any current masthead page.

OM960663I

Downloaded by CARLI CONSORTIUM on June 30, 2009
Published on March 4, 1997 on http://pubs.acs.org | doi: 10.1021/om960663i

(49) Altomare, A.; Cascarano, G.; Giacovazzo, C.; Guagliardi, A. *J. Appl. Crystallogr.* **1994**, *27*, 435.

(50) Flack, H. D. *Acta Crystallogr.* **1983**, *A39*, 876.

(51) Ammeter, J. H.; Bürgi, H. B.; Thibeault, J. C.; Hoffmann, R. *J. Am. Chem. Soc.* **1978**, *100*, 3686.

(52) Alvarez, S. *Table of Parameters for Extended Hückel Calculations*; Departamento de Química Inorgánica, Universidad de Barcelona: Barcelona, Spain, 1989.